ELSEVIER

NeuroImage

www.elsevier.com/locate/ynimg
NeuroImage 22 (2004) 409–418

Limbic–frontal circuitry in major depression: a path modeling metanalysis

D.A. Seminowicz,[a] H.S. Mayberg,[a,*] A.R. McIntosh,[a] K. Goldapple,[a] S. Kennedy,[b] Z. Segal,[b] and S. Rafi-Tari[b]

[a] *Rotman Research Institute, Baycrest Centre for Geriatric Care, Toronto, Ontario M6A 2E1, Canada*
[b] *Centre for Addiction and Mental Health, Toronto, ON, Canada*

Received 16 October 2003; revised 13 December 2003; accepted 13 January 2004

This paper reports the results of an across lab metanalysis of effective connectivity in major depression (MDD). Using FDG PET data and Structural Equation Modeling, a formal depression model was created to explicitly test current theories of limbic–cortical dysfunction in MDD and to characterize at the path level potential sources of baseline variability reported in this patient population. A 7-region model consisting of lateral prefrontal cortex (latF9), anterior thalamus (aTh), anterior cingulate (Cg24), subgenual cingulate (Cg25), orbital frontal cortex (OF11), hippocampus (Hc), and medial frontal cortex (mF10) was tested in scans of 119 depressed patients and 42 healthy control subjects acquired during three separate studies at two different institutions. A single model, based on previous theory and supported by anatomical connectivity literature, was stable for the three groups of depressed patients. Within the context of this model, path differences among groups as a function of treatment response characteristics were also identified. First, limbic–cortical connections (latF9-Cg25-OF11-Hc) differentiated drug treatment responders from nonresponders. Second, nonresponders showed additional abnormalities in limbic–subcortical pathways (aTh-Cg24-Cg25-OF11-Hc). Lastly, more limited limbic–cortical (Hc-latF9) and cortical–cortical (OF11-mF10) path differences differentiated responders to cognitive behavioral therapy (CBT) from responders to pharmacotherapy. We conclude that the creation of such models is a first step toward full characterization of the depression phenotype at the neural systems level, with implications for the future development of brain-based algorithms to determine optimal treatment selection for individual patients.

Keywords: Human; Brain; Cingulate; Frontal; Hippocampus; Thalamus; Depression; Treatment; PET; FDG; Metabolism; Multivariate; Network; Structural equation modeling

Introduction

To test a previously proposed limbic–cortical network model developed with positron emission tomography (PET) measures of brain glucose metabolism (see Fig. 1), we present findings of an across-lab metanalysis examining effective connectivity in major depression (MDD) using Structural Equation Modeling.

Depression is a common affective disorder characterized by persistent negative mood and selective deficits in cognitive, circadian, and motor functioning. Neuroimaging studies of both cerebral blood flow (CBF) and glucose metabolism (FDG) have repeatedly identified regional abnormalities in the untreated depressed state (Baxter et al., 1989; Bench et al., 1992; Drevets et al., 1992; Mayberg et al., 1994). Consistently reported are frontal and cingulate changes. While less common, other limbic and subcortical regions including hippocampus, amygdala, posterior cingulate, striatum, and thalamus are also implicated. Frontal and cingulate changes involve multiple but distinct sites, with anatomical convergence across functional, structural, and post-mortem pathological studies: dorsolateral (BA9/46) and ventrolateral prefrontal cortex (BA10/47), dorsomedial and ventromedial frontal cortex (BA9/10/11/32), and dorsal, rostral, and subgenual cingulate (BA24b, 24a, 25). In addition to abnormalities identified in the pretreatment depressed state, changes in many of these same regions are seen with various types of pharmacological, cognitive, and somatic antidepressant treatments (Brody et al., 1999, 2001; Goldapple et al., 2003; Kennedy et al., 2001; Mayberg et al., 2000; Pizzagalli et al., 2001a).

While there is growing consensus that an array of brain areas are involved in depression, not all regions are reported in all studies. Furthermore, there is variability in the direction of CBF and FDG changes, particularly in those areas of frontal and anterior cingulate cortex considered most critical. Our own studies, as well as others (Brannan et al., 2000; Pizzagalli et al., 2001a), demonstrate distinct differences in anterior cingulate activity that distinguish eventual responders and nonresponders scanned before pharmacotherapy (Mayberg et al., 1997; Wu et al., 1999). As well, change patterns in responders and nonresponders to identical treatment show mirror metabolic change patterns in certain specific regions, including regions unaffected in the baseline state (i.e., posterior cingulate, and hippocampus). In addition, there are clear regional change pattern differences across unique treatments (CBT, medication, ECT) affecting similar regions in different ways (i.e., frontal decreases and hippocampal increases with CBT; frontal increases and hippocampus decreases with pharmacotherapy; decreases in both with ECT) (Buchsbaum et al., 1997; Goldapple et al., 2004; Henry et al., 2001; Kennedy et al., 2001; Martinot et al., 1990; Mayberg, 2003;

* Corresponding author. Baycrest Centre for Geriatric Care, Rotman Research Institute, 3560 Bathurst Street, Toronto, Ontario, Canada M6A 2E1. Fax: +1-416-785-2862.
E-mail address: hmayberg@rotman-baycrest.on.ca (H.S. Mayberg).
Available online on ScienceDirect (www.sciencedirect.com.)

1053-8119/$ - see front matter © 2004 Elsevier Inc. All rights reserved.
doi:10.1016/j.neuroimage.2004.01.015

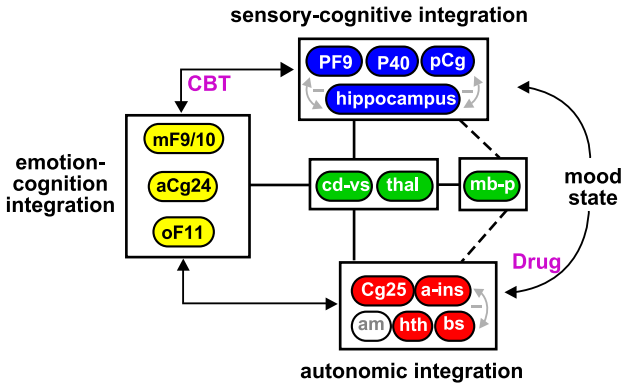

Fig. 1. Limbic–cortical dysregulation model. Regions with known anatomical interconnections are grouped into four main behavioral compartments. The cortical limbic (dorsal–ventral) segregation within each 'compartment' additionally identifies those brain regions where an inverse relationship is seen across the different PET paradigms. Sadness and depressive illness are both associated with decreases in dorsal neocortical regions (sensory-cognitive compartment) and relative increases in ventral limbic and paralimbic areas (autonomic compartment). The model, in turn, proposes that illness remission occurs when there is appropriate modulation of dysfunctional limbic–cortical interactions (small grey arrows)—an effect facilitated by various forms of treatment (purple). Abbreviations: mF = medial prefrontal; aCg = rostral anterior cingulate; oF = orbital frontal; cd-vs = caudate-ventral striatum; thal = thalamus; mb-p = midbrain-pons; Cg25 = subgenual cingulate; a-ins = anterior insula; am = amygdala, hth = hypothamus; bs = brainstem; PF = dorsolateral prefrontal; p = parietal; pCg = posterior cingulate. Numbers: Brodmann designations.

Nobler et al., 2001). Unique treatment-specific effects are also seen; notably brainstem and thalamic changes with medication and medial and orbital frontal changes with CBT. In general, subdivisions of cingulate, frontal cortex, hippocampus, and thalamus figure predominantly across all studies.

The nature of these reported changes suggests a complex interaction between the pre-treatment brain state, brain responsivity, and different treatment interventions that is not intuitive. Nonetheless, the findings suggest a testable hypothesis that variations in the state of connections across a set of critical regions (effective connectivity), as measured using a multivariate technique, might better explain the reported variability across independent depression patient treatment samples than the more typical approaches examining relative differences in discrete regions among groups (change distribution analysis, SPM) (Friston, 1994; Horwitz et al., 1999).

To provide further theoretical context for such an approach, a major depressive episode is considered, at the brain level, the net result of maladaptive functional interactions among a highly integrated network of limbic–cortical regions normally responsible for maintaining homeostatic emotional control in response to cognitive and somatic stress (Mayberg, 2003; McEwen, 2003). Network dysfunction combined with variations in active intrinsic compensatory processes might therefore account for heterogeneity of depressive symptoms observed clinically, as well as variations in pretreatment scan patterns described experimentally. Non-imaging studies implicate various contributors to these adaptive differences including genetic vulnerability, affective temperament, and developmental insults and environmental stressors (Bagby et al., 2003; Caspi et al., 2003; Heim and Nemeroff, 2001). Treatments for depression can be similarly viewed within such a systems framework, whereby different modes of treatment facilitate recovery via initiation of additional adaptive chemical and molecular changes (Hyman and Nestler, 1996; Vaidya and Duman, 2001). Progressively, more aggressive treatments needed to ameliorate symptoms in some patients may reflect poor adaptive capacity of this network in these patient subgroups.

To fully test such hypotheses, baseline patterns in patients with known clinical response to various treatments are first required. In addition, a more deliberate assessment of these state–region–treatment interactions is needed. The multivariate technique partial least squares (PLS) combined with structural equation modeling provides one such approach (Horwitz et al., 1999; McIntosh, 2000; McIntosh and Gonzalez-Lima, 1994), whereby relationship between regions in a defined theoretical model can be tested across different patient cohorts where variations in treatment response are known.

This study had three main goals. The first and most critical was to create a formal depression model structure that would both represent our previous theoretical construct (Fig. 1) and show specificity and good reliability across multiple depressed patient samples. The second was to characterize path differences within such a model that would distinguish responders from nonresponders. Third, differences associated with response to different treatments were considered. We hypothesized that the combined use of PLS and SEM, constrained by an a priori focus on those brain regions consistently identified in past studies, and knowledge of known anatomical connections among these specified regions would identify such a model. It was further hypothesized that paths involving anterior cingulate would be critical to responder–nonresponder differences. While the design of this study is largely exploratory, it is seen as the first step to establishing a simplified model system for future prospective studies.

Methods

Subjects

This metanalysis combined resting state FDG-PET data from independent studies performed at two institutions (University of

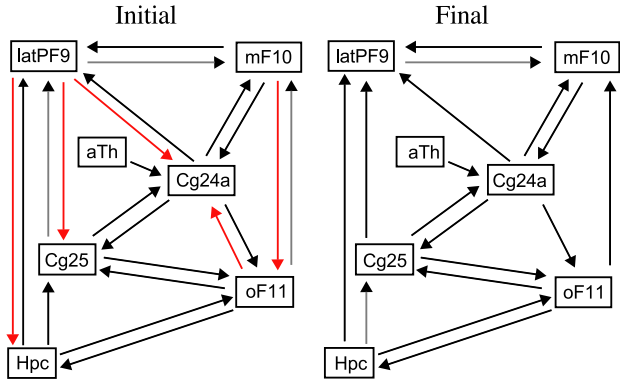

Fig. 2. Initial anatomically derived model (left) and final "best" model. Several paths in the initial model were modified (RED) to get the best stability for all depressed cohorts, giving the final model. The regions shown are derived from repeated findings in the depression and emotion imaging studies, and are aligned in a manner that reflects the theoretical model in Fig. 1. Anatomical connections were derived from converging results from primate, rat, and human studies. Path coefficients for the final model for each group independently are given in Tables 3 and 4.

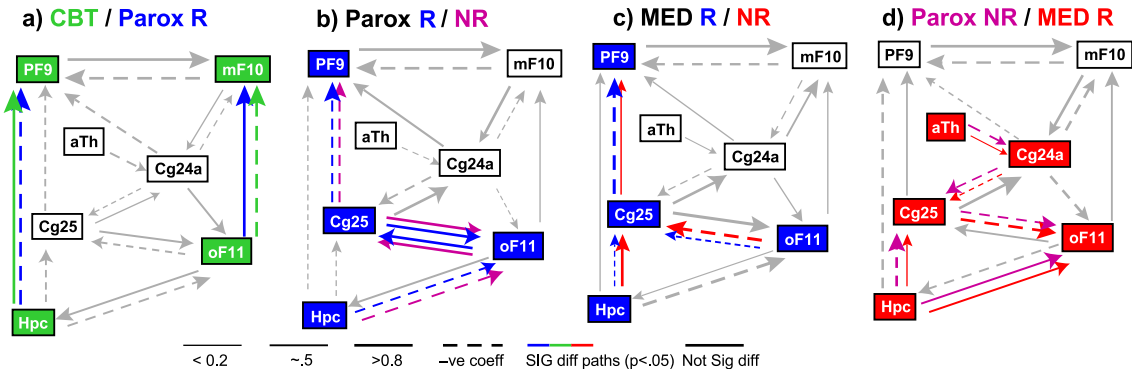

Fig. 3. Path diagrams for various comparisons. (a) CBT vs. Parox (n = 27); (b) Parox responders vs. nonresponders (n = 69); (c) MED responders vs. nonresponders (n = 36); (d) MED nonresponders vs. Parox nonresponders (n = 32). Approximate path weights are shown by the width of the lines, with solid lines indicating positive, and broken lines negative path coefficients. Colored lines indicate significantly different paths between the groups compared and the colors of the paths match the colors of the groups, listed above each comparison. The analysis of Parox-R to MED-R revealed no significant differences.

Texas Health Sciences Center at San Antonio and the University of Toronto). All data were acquired using similar recruitment inclusion and exclusion criteria and a comparable imaging protocol on a similar generation PET scanner and were thus, considered comparable for the proposed cross-group analyses. Baseline, pre-treatment scans from 119 patients with major depression were collated from these three distinct, unrelated depression imaging studies (two in Toronto, one in San Antonio). Two groups of healthy controls (San Antonio, n = 17, Toronto, n = 25) were also included. All studies involved a single FDG-PET scan acquired before initiation of antidepressant treatment.

Three principle cohorts were designated based on the source of the original data. The two Toronto groups were composed of patients who had participated in separate controlled clinical treatment trials. These patients were recruited by advertisement to receive a specific antidepressant treatment administered using a standardized protocol: Group 1 (Toronto, n = 69; Kennedy et al., 2001) received 6 weeks of outpatient treatment with the antidepressant paroxetine (Parox). Group 2 (Toronto, n = 14; Goldapple et al., 2004) recruited as part of a separate study, received a 15-week outpatient course of cognitive behavioral therapy (CBT). Group 3 was composed of patients referred by their physicians from a tertiary, University Medical School mood disorders clinic for the express purpose of studying resting metabolism in untreated major depression (San Antonio, n = 36; Brannan et al., 2000; Mayberg et al., 1997). This group, while not formally recruited for a specific treatment, received antidepressant medication following scanning, selected by the treating clinic psychiatrist (MED). Patients in all three cohorts met standardized criteria for a current major depression episode (unipolar type), and all were drug-free at the time of scan acquisition. Baseline severity of depression was rated using the Hamilton Depression Rating Scale 17-item (HDRS) in all subjects at the time of the PET scan.

Of the total sample, 104 (87.4%) were male and 15 (12.6%) were female, with an average age of 39.8 ± 9.96 years (mean ± SD; range age 20–62). Other clinical and demographic characteristics are shown in Table 1. Treatment outcomes were available for all subjects, and each cohort was divided into two groups, responders (R) or nonresponders (NR) based on one of two criteria: a minimum 50% drop in HDRS scores at the end of the formal treatment trial (CBT, Parox groups) or consensus evaluations of two independent psychiatrists in a retrospective chart review covering the 2 months following scanning (MED group). The two methods were cross-validated in a subsample of the MED group who were additionally involved in a specific trial of fluoxetine (Brannan et al., 2000).

PET imaging and data preprocessing

Resting state (eyes closed, quiet room, no task) cerebral glucose metabolism was measured using ^{18}[F]-deoxyglucose positron emission tomography (FDG-PET) in all subjects. Two scanners of comparable generation and resolution were used: a GEMS 2096 in Toronto and a GE-Scanditronix 4096 camera in San Antonio. Both cameras have a 15-slice, 10-cm field of view and 6.5 center-to-center interslice distance. Measured attenuation was performed at both sites. Raw scans from all subjects from both scanners were re-reconstructed to an initial in-plane resolution of 7.0-mm full width at half maximum for the expressed purpose of this metanalysis. Reconstructed scan data was then spatially

Table 1
Cohort characteristics, means with standard deviations

	CBT	Parox-R	Parox-NR	MED-R	MED-NR
N	14	53	16	21	15
Males/females	6/8	53/0	16/0	16/5	20/1
Age	40.7 ± 9.1	37.3 ± 10.1	37.8 ± 10.5	42.7 ± 8.8	46.3 ± 7.9
Ham-D pre	20.1 ± 2.8	23.4 ± 3.2	22.7 ± 3.2	19.9 ± 3.5	21.3 ± 5.0
Ham-D post	6.71 ± 4.2	6.15 ± 3.6	17.9 ± 4.5	–	–

normalized to standard 3D-coordinate space in SPM99 (Friston et al., 1995) using the SPM95 template, interpolated to 2 × 2 × 4 mm voxels. Smoothing was done with a 12-mm FWHM Gaussian kernel.

Structural equation modeling

SEM involved the following steps. First, a set of candidate regions was chosen for model construction, based on published findings. An anatomically defined model was prescribed using these regions, and SEM was used to test the fit of this specified model. The goal was to design a model that would fit all three depressed cohorts independently. Once such a model was identified that satisfied all requirements (stable among all cohorts and anatomically accurate), the model was applied simultaneous to the three primary cohorts and then to treatment-type and response-outcome subgroups within and across cohorts for comparisons at two levels. The first level tested whether there were differences among the groups overall. The second level determined which paths were most critical to any identified model differences.

Region selection

Region selection was both theory and data-driven. While an ideal model would theoretically involve all brain regions shown in the accumulated depression literature, region number was intentionally limited to ensure parsimony (model simplicity). Since parsimony will generally increase the reliability of a model, we began with a set of regions identified in previous analyses of these specific data sets (Goldapple et al., 2004; Kennedy et al., 2001; Mayberg et al., 1997) that also overlapped other published findings (Arango et al., 1999; Auer et al., 2000; Biver et al., 1994; George et al., 1994; Hornig et al., 1997; Liotti and Mayberg, 2001; Manji et al., 2001; Sheline et al., 1996; Smith et al., 1999; Starkstein et al., 1987), optimizing the likelihood of accounting for expected variance among the depressed groups. Areas selected were dorsolateral prefrontal Brodmann areas BA 9 (latF9), orbital frontal BA 11 (OF11), medial frontal BA 10 (mF10), subgenual cingulate BA 25 (Cg25), rostral cingulate BA 24a (Cg24a), hippocampus (Hc), and anterior thalamus (aTh). Consistently, these regions are identified in functional as well as structural and postmortem mood disorder studies, including comparisons of patients and controls (latF9, Cg24, OF11, mF10; Baxter et al., 1989; Bench et al., 1993; Drevets et al., 1997; Mayberg et al., 1997; Rajkowska, 2000), treatment effects (latF9, aTh, Cg25, OF11, mF10; (Buchsbaum et al., 1997; Kennedy et al., 2001; Mayberg et al., 2000; Saxena et al., 1999), and response prediction (Cg24; (Kennedy et al., 2001; Mayberg et al., 1997; Wu et al., 1999). Further, these areas are seen in sad mood provocation studies in both normal and depressed subjects (Cg25, lat9, mF10, OF11, Cg24, aTh; (e.g., Damasio et al., 2000; George et al., 1995, 1997; Liotti et al., 2002; Mayberg et al., 1999), as well as studies of emotional monitoring and self-reference (Cg24, mF10, OF11; Davidson, 2001; Elliott et al., 2000; Fossati et al., 2003; Zald et al., 2002). While additional regions, such as the amygdala, caudate, posterior cingulate, and parietal cortex, could also have been included based on reports, we focused on this more limited region set to meet the parsimony objective, and also test most directly our previously postulated depression model (Mayberg, 1997, 2002b) (Fig. 1).

To both confirm the appropriateness of these regions in building the depression model to be tested, and to refine the voxel selection for each region to be used in the path analysis, all 119 patients were combined and compared to all controls (n = 42) in a partial least squares (PLS) analysis (see McIntosh et al., 1996 for description of PLS), run in Matlab (Mathworks Inc., MA). PLS outputs a covariance map of functional connectivity, thus refining the location of regions belonging to the common network that distinguishes depressed patients from healthy controls, most generally. That is, the comparison showed a covariance pattern based on the contrast of controls and patients similar to how a univariate analysis would compare two groups. This analysis identified a network involving all of the regions identified above (data not shown). Identified in this analysis, but not included in our model, were caudate, parietal cortex, insula and posterior-cingulate. Notably, the amygdala was not seen in the PLS analysis.

Peak salience voxels for selected regions—targeted a priori—were chosen from this Group PLS analysis. Voxel values for each coordinate were extracted from the data set of each subject. For each region, bilateral and generally symmetrical significant voxels were available. The maximum peak voxel for each region was used, regardless of hemisphere. All regions selected were right-sided except for lateral BA9. Right and left BA9 were highly intercorrelated, and replacement of the left-sided region with the right-sided gave very similar results overall. We present only the model using the left-sided region, selected based on its higher salience. The coordinates are shown in Table 2.

Model construction

A model was defined based on previous findings and published theory as described above, in combination with known anatomical connections between these specified limbic and frontal lobe regions (e.g., Carmichael and Price, 1994, 1995; Cavada et al., 2000; Ferry et al., 2000; Freedman et al., 2000; Haber et al., 1995; Kunishio and Haber, 1994; Morris et al., 1999; Petrides and Pandya, 1984, 1994; Ray and Price, 1993; Shumake et al., 2000; Vogt and Pandya, 1987; Vogt et al., 1992). Excitatory and inhibitory paths were not explicitly designated. Rather presence (or absence) of known tracts (unidirectional, bi-directional, or reciprocal) connecting two specific sites was defined. The initial model (Fig. 2, left) was modified stepwise (i.e., removing and adding connections path-by-path), guided by anatomic 'truth' to obtain a model that was stable for all depressed cohorts. After each path modification, model stability was retested. Whether the model adequately defined a network for a given group was determined based on the fit difference between the test model (created) and an independence model, in which all regions are assumed to be independent of each other (i.e., no connection). Model construction

Table 2
Regions used in model and their Talairach coordinates

Region name (Brodmann's area)	Talairach coordinate (x, y, z)
Hippocampus	22, −14, −16
Orbital frontal cortex (11)	2, 28, −20
Medial frontal cortex (10)	16, 64, −4
Lateral prefrontal cortex (9)	−28, 34, 32
Rostral anterior cingulate (24a)	2, 32, 4
Subgenual cingulate (25)	8, 16, −8
Anterior thalamus	2, −6, 4

was aimed at creating a model that attained good stability for all depressed groups and was as close as possible to the initial model.

Planned contrasts

To understand potential differences among groups of potential relevance to group membership, treatment selection bias, and treatment response, planned contrasts examined (1) main effect of group (Parox69 vs. CBT13 vs. MED36; (2) main effect of Response (within group: Parox-R vs. NR; MED-R vs. NR; note, there were no CBT NR available); and (3) response−group interactions (Parox-R vs. MED-R; Parox-R vs. CBT-R; Parox-NR vs. MED-NR).

Path analysis

Path analysis was carried out using SEM implemented in AMOS (Version 4, SmallWaters Co.). SEM applied to functional neuroimaging data can generally be summarized as a three-step process, whereby a covariance matrix is determined from the sample regions and applied to a defined model (described above), such that a weight (path coefficient) is calculated for each path in the model (Buchel and Friston, 1997; Horwitz et al., 2000; McIntosh, 2000; McIntosh and Gonzalez-Lima, 1994; Nyberg et al., 1996). The causal structure of the model is defined by consulting the neuroanatomy literature. This anatomical structure is constrained across groups and tasks, and the emphasis is on whether there are statistically significant changes in the path coefficients between conditions. In this context, the goodness or badness of fit is not an issue (McIntosh, 1999).

Since regions and paths of potential importance to the characterization of a depression circuit were excluded (due to sample size and maintaining parsimony), residuals (error terms that could account for these extraneous sources of variance) were included. The weightings of the influence of residuals on nodes were constrained to 35%, so that most of the variance is forcedly accounted for from within the model (McIntosh and Gonzalez-Lima, 1994). To improve model stability, paths that had absolute coefficients of

Table 3
Path coefficients (estimate), standard error (SE), critical ratio (CR), and *P* value (*P*) for each path by group

	Parox-R				Parox-NR			
	Estimate	SE	CR	*P*	Estimate	SE	CR	*P*
aThal→r24a	−0.273	0.123	−2.211	0.027	−0.798	0.239	−3.343	0.001
Hc→BA11	−0.637	0.206	−3.086	0.002	0.96			
BA11→Hc	0.585	0.167	3.509	0	−0.404	0.206	−1.967	0.049
m10→Lat9	0.96				−0.96			
Lat9→m10	−0.808	0.186	−4.347	0	0.929	0.272	3.418	0.001
BA25→Lat9	−0.611	0.273	−2.237	0.025	0.13	0.293	0.444	0.657
r24a→Lat9	0.273	0.176	1.555	0.12	−0.244	0.278	−0.876	0.381
r24a→m10	−0.086	0.158	−0.543	0.587	−0.34	0.26	−1.305	0.192
m10→r24a	0.798	0.289	2.762	0.006	0.96			
r24a→BA11	−0.243	0.179	−1.358	0.175	−0.031	0.4	−0.077	0.939
BA11→m10	0.432	0.14	3.076	0.002	0.572	0.241	2.373	0.018
BA11→BA25	0.138	0.159	0.87	0.384	−0.011	0.423	−0.027	0.978
BA25→BA11	0.96				0.151	0.493	0.306	0.759
r24a→BA25	−0.587	0.145	−4.055	0	−0.621	0.32	−1.942	0.052
BA25→r24a	0.96				0.725	0.333	2.177	0.029
Hc→BA25	−0.028	0.194	−0.145	0.885	0.261	0.641	0.408	0.683
Hc→Lat9	−0.127	0.193	−0.656	0.512	−0.989	0.412	−2.4	0.016
	MED-R				MED-NR			
	Estimate	SE	CR	*P*	Estimate	SE	CR	*P*
athal→r24a	−0.184	0.242	−0.76	0.447	0.117	0.216	0.542	0.588
Hc→BA11	−1.001	0.343	−2.92	0.004	0.694	0.398	1.744	0.081
BA11→Hc	0.332	0.259	1.28	0.2	−0.42	0.665	−0.631	0.528
m10→Lat9	0.988	0.385	2.57	0.01	0.96			
Lat9→m10	−0.771	0.341	−2.263	0.024	−0.62	0.312	−1.988	0.047
BA25→Lat9	−0.896	0.546	−1.642	0.101	0.211	0.568	0.371	0.711
r24a→Lat9	0.369	0.283	1.304	0.192	0.022	0.382	0.057	0.955
r24a→m10	0.331	0.269	1.228	0.219	0.35	0.337	1.038	0.299
m10→r24a	−0.203	0.435	−0.467	0.641	−0.826	0.742	−1.114	0.265
r24a→BA11	0	0.245	0	1	−0.484	0.304	−1.592	0.111
BA11→m10	0.33	0.218	1.515	0.13	−0.429	0.385	−1.112	0.266
BA11→BA25	−0.197	0.255	−0.772	0.44	0.561	0.385	1.456	0.145
BA25→BA11	0.96				−0.96			
r24a→BA25	−0.352	0.254	−1.383	0.167	0.082	0.377	0.217	0.828
BA25→r24a	0.96				0.96			
Hc→BA25	−0.201	0.316	−0.636	0.525	0.172	0.496	0.347	0.728
Hc→Lat9	0.045	0.29	0.154	0.878	0.073	0.329	0.222	0.824

P-value are for each path, and are not related to X^2_{diff} between group. Estimates are for each group separately and not constrained between group.

greater than 1 were fixed at ± 0.96, since a path coefficient of greater than 1 is theoretically impossible (implies over 100% of variance accounted for).

Lastly, because paths reflect a direct influence of one region on another, negative path coefficients are interpreted to indicate ensemble inhibition, and positive paths net excitation. We submit, however, that this interpretation does not necessarily reflect activity at the cellular level, but simply the interactions between regions based on measured total regional metabolic activity (Nyberg et al., 1996).

To compare the groups, a *stacked model* method was employed (McIntosh and Gonzalez-Lima, 1994). In the *null model*, all parameter estimates (path coefficients) are set equal across groups. In the *alternative model*, no paths are constrained across groups. An *omnibus* test (null vs. alternative) was then performed and statistical significance is determined by comparison of X^2 (X^2_{diff}) values of fit. If the alternative model differs significantly from the null, it can be concluded that the groups differ significantly in the context of the prescribed model. When this occurs, stepwise comparisons of individual paths are then performed between groups to determine more precisely which paths are responsible for the significant difference in the omnibus.

Results

A single model was created for all three depressed cohorts based on the criteria for model construction given above. Within the context of this model, paths differentiating groups as a function of treatment–response interactions were also identified, but not differences due to either cohort site (Toronto vs. San Antonio) or the specific treatment alone (Drug vs. CBT).

Model fit and overall group differences

The initial test model and the modified best-fit final model are shown in Fig. 2. Specificity of this model for depressed patients was inferred by failure of the data from either control group to fit the prescribed model. A better fit for the independence model (i.e., no relationship between variables) was seen in these non-depressed control samples. There were no significant differences in the overall model as a function of test site (Toronto vs. San Antonio: MED vs. CBT or Parox) or Treatment Group (MED vs. Parox; MED vs. CBT, CBT vs. Parox).

Responder/nonresponder differences, within group

Paroxetine group

In the Parox group, 52 patients were treatment responders (R) and 17 were nonresponders (NR). Full model contrasts of these subgroups demonstrated significant differences ($X^2_{\text{diff}}(12) = 54.14$, $P < 0.00001$) (Table 3, columns 1 and 2). Systematic comparisons of individual paths identified a specific effective connectivity pattern that best explained the R–NR differences involving paths hc→OF11↤Cg25→latF9 ($X^2_{\text{diff}}(4) = 37.71$, $P < 0.00001$) (Fig. 3b).

Medication group

A similar analysis was performed on the San Antonio sample (medication treatment (MED), physicians' choice). This group consisted of 21 responders and 15 nonresponders. Overall, the two subgroups showed a trend toward significance differences (X^2_{diff} (10) = 16.51, $P < 0.10$) (Table 3, columns 3 and 4). Therefore, the patterns of paths that showed the most significant differences were examined and included Hc→Cg25, and OF11→Cg25→latF9, ($X^2_{\text{diff}}(3) = 12.17$, $P < 0.010$) (Fig. 3c). This pattern is remarkably similar to those discriminating R and NR in the Parox group, despite differences in site of acquisition, recruitment strategy, and method of defining response.

Between-group differences

To further explore the nature of R–NR differences in the above subgroups, R and NR were also compared across sites. Parox-R compared to MED-R showed no significant differences (X^2_{diff} (14) = 14.92, $P = 0.383$). This finding again confirms an unlikely influence of scan acquisition site, scanner, or method of recruitment in explaining R–NR differences in the Parox or MED groups.

Table 4
Path coefficients (estimate), standard error (SE), critical ratio (CR), and *P* value (*P*) for each path by group

	Parox13				CBT			
	Estimate	SE	CR	*P*	Estimate	SE	CR	*P*
aThal→r24a	−0.96				−0.231	0.326	−0.71	0.478
Hc→BA11	−0.96				−0.96			
BA11→Hc	0.437	0.21	2.076	0.038	0.347	0.244	1.423	0.155
m10→Lat9	−0.96				−0.96			
Lat9→m10	0.96				0.958	0.324	2.957	0.003
BA25→Lat9	0.241	0.469	0.515	0.607	0.142	0.29	0.491	0.623
r24a→Lat9	−0.074	0.278	−0.268	0.789	0.167	0.293	0.571	0.568
r24a→m10	−0.172	0.26	−0.66	0.509	−0.329	0.29	−1.134	0.257
m10→r24a	0.96				0.782	0.609	1.285	0.199
r24a→BA11	0.161	0.272	0.591	0.554	0	0.3	−0.001	0.999
BA11→m10	−0.007	0.238	−0.03	0.976	−0.998	0.338	−2.948	0.003
BA11→BA25	−0.215	0.234	−0.918	0.358	0.171	0.343	0.498	0.618
BA25→BA11	0.96				0.408	0.374	1.09	0.276
r24a→BA25	−0.722	0.265	−2.729	0.006	0.346	0.412	0.84	0.401
BA25→r24a	0.96				0.056	0.344	0.164	0.87
Hc→BA25	−0.96				0.485	0.446	1.088	0.277
Hc→Lat9	−0.96				0.033	0.412	0.08	0.937

P values are for each path, and are not related to X^2_{diff} between groups. Estimates are for each group separately and not constrained between groups.

Parox-NR vs. MED-NR, however, differed significantly overall (X^2_{diff} (13) = 27.43, $P < 0.02$) and post hoc pathwise comparisons revealed significant differences in paths Hc→OF11, Hc→Cg25→OF11, aThal→Cg24→Cg25, (X^2_{diff} (5) = 20.09, $P < 0.001$) (Table 3, columns 2 and 4) (Fig. 3c).

Treatment–response interactions, within site

CBT vs. Parox (comparable recruitment, specified treatment protocol)

Lastly, to evaluate potential path differences that distinguish eventual pharmacotherapy responders from cognitive therapy responders, controlling for site of scan acquisition, mode of recruitment, and method of response assessment, the CBT group ($n = 14$) and a subset of the Parox group ($n = 13$) were compared. Previously reported from these subgroups are pre–post-treatment metabolic changes unique to treatment: Cg24 and hippocampal increases and mF10, OF11, and latF9 decreases with CBT and latF9 increases and Cg25 decreases with paroxetine (Goldapple et al., 2003). There was a significant difference between the groups in the model overall (X^2_{diff} (7) = 20.53, $P < 0.005$). Specific paths accounting for these differences involved Hc→latF9, and OF11→mF10 (X^2_{diff} (2) = 11.10, $P < 0.005$), with path coefficients −0.05 and −0.94, respectively, for CBT, and −0.96 and −0.05, respectively, for Parox (Fig. 3a). Further, when pre- and post-treatment scans were additionally compared for each group separately (CBT-pre vs. CBT-post; Parox-pre vs. Parox-post), significant path differences were found from Hc→latF9 in the Parox group and OF11→mF10 in the CBT group (among other paths), resulting in a reversal of aberrant pathways in distinguishing the two groups (data not shown). Table 4 shows the path data for the above groups independently.

Discussion

These findings define, using structural equation modeling of resting state FDG-PET scan data, patterns of effective connectivity that differentiate distinct groups of unmedicated unipolar depressed patients. Furthermore, specific cortical–cortical, cortical–limbic, and limbic–subcortical path interactions within this specified depression model distinguished patient subgroups. Most interestingly, these differences were not simply gross cohort differences, but rather more complex interactions reflecting both treatment type and response outcome. Rather than providing evidence for a depression phenotype, this modeling approach appears most sensitive to identifying treatment–response interactions, findings not apparent from univariate analyses between groups. For example, univariate analyses showed Parox and CBT had general frontal hypermetabolism, while MED patients had frontal hypometabolism (Goldapple et al., 2004; Mayberg et al., 1997, 2000). Despite these differences, perhaps reflecting multiple depression phenotypes, only in the modeling analyses was it evident that regional interactions separated groups by treatment response. Validation of this method for use in response prediction will require prospective studies where patient characteristics are considered in the model construction.

Overall, there were several clear trends. Drug responders across cohorts (both Parox and MED groups) differed from nonresponders in a network subsystem involving both limbic afferents and cortical efferents of area 25 (Figs. 3b, c). Additional differences between drug nonresponders across treatment groups were seen in contiguous cingulo-subcortical pathways (Th-cg24a-25) (Fig. 3d). A third distinct fronto-frontal (mF10–OF11) pattern distinguished CBT-responsive patients from medication responders (Fig. 3a).

In support of a consistent 'drug-responsive' brain type was the lack of a significant model difference in the analysis of the Parox responders vs. MED responders, despite clear differences in site of scan acquisition, scanner, and recruitment methods. These similarities in overall model configuration are hypothesized to reflect comparable adaptive changes not present in nonresponders in either drug-treatment cohort (Koob and Le Moal, 2001; Mayberg, 2002b). While integral to the model construction in each cohort, pathways involving BA24 were not critical for distinguishing responders from nonresponders except in the most treatment nonresponsive group—an apparent contradiction to previous reports of R–NR differences using alternative univariate methods (Kennedy et al., 2001; Mayberg et al., 1997; Pizzagalli et al., 2001b; Wu et al., 1999), likely explained by inherent differences between univariate and multivariate approaches. The additional involvement of hippocampus and BA11 in NR is particularly interesting, as these regions show cellular morphometric and biochemical changes in post-mortem studies (Harrison, 2002; Mann et al., 1996; Rajkowska, 2000) are known targets of classic antidepressant drugs (Blier and Bouchard, 1994; Blier and de Montigny, 1985; Duman et al., 1999; Mann et al., 1995) and are implicated in control of endocrine/autonomic responses in various genetic, developmental, and environmental stress models (e.g., through connections to amygdala, periaqueductal gray, and hypothalamus) (McEwen et al., 1968; Plotsky et al., 1998; Sapolsky, 2000). These regions have been further linked to emotional/evaluative learning, hedonic, and reward responses and affect–cognitive interactions through connections to adjacent areas of orbitofrontal and medial frontal cortices (see Devinsky et al., 1995 for review; An et al., 1998; Charara and Grace, 2003; Dias et al., 1996; Drevets et al., 1992; Elliott, 1998; Elliott et al., 2002; Keightley et al., 2003; Liotti et al., 2002; Mayberg, 2002a; Schultz et al., 2000; Vogt et al., 1992; Zald et al., 2002), behaviors prominently affected in major depression.

In contrast, comparison of the two NR groups revealed additional limbic–subcortical changes (thalamus, 24, 25) suggestive of graded involvement of these pathways in these two groups. While there were no specific behavioral or severity measures that explained these differences, the MED-NR group had more patients receiving multiple medications in the period used to document response status, suggesting more severe illness not captured by total number of previous episodes or Hamilton scores. This is not atypical of a tertiary care, subspecialty depression clinic population. That said, in spite of these limbic–subcortical differences, similar limbic–cortical interactions were present in both groups, accounting for the primary discriminator between R and NR.

These unique limbic–subcortical (25–th–24) abnormalities in the MED nonresponder group in the context of apparent non-involvement of either cortical–limbic or cortical–cortical pathways is consistent with both the historical and emerging literature on treatment of refractory depression. Notably, surgical interventions used to treat such patients (cingulotomy, anterior capsulotomy, subcaudate tractotomy) are thought to disrupt these same cingulo-subcortical pathways (cf. Cosgrove and Rauch, 1995, 2003; Malhi and Bartlett, 2000). This hypothesis is further supported by more recent evidence demonstrating significant correla-

tions between elevated pretreatment cingulate 25 activity and response to cingulotomy (Dougherty et al., 2003).

In contrast, the CBT responder group (compared to a subset of the Parox responder group) was distinguished by the absence of limbic or subcortical pathway involvement, despite similarities in demographics, recruitment methods, and disease characteristics (Fig. 3a). In keeping with recent theories of dysregulated homeostatic responses to ongoing stress (McEwen, 2003; McEwen and Wingfield, 2003), the more restricted fronto-frontal abnormalities in the CBT group may reflect a preserved compensatory capacity not seen in patients requiring medication where cortical–limbic dysregulation is apparent. While speculative, this interpretation is nonetheless consistent with clinical observations and past classification strategies distinguishing "reactive" from "endogenous" types of depression (Klein, 1974).

There are several limitations to these results. First, this is a retrospective meta-analysis. A prospective large scale study, controlled for illness severity, recruitment strategy, treatment assignment method, outcome instruments as well as gender, age, and other demographic and disease-specific variables are needed using a comparable analytic approach. In addition, temporal stability, (within-subject reliability over time), treatment randomization, sample size, and analytical bias (model assumptions) will need to be explicitly considered.

A second limitation concerns the derived model. While we recognize that there are regions implicated in the depression network as well as other existing anatomical pathways not included in the model, we have created a testable model that we feel is sufficient to explain various aspects of depression pathology. As with any study, this model should be tested further, preferably both within and across subjects and groups (Boomsma, 2000). The application of this approach and its inherent limitations is not limited to FDG PET data; blood flow PET, perfusion MRI, and resting BOLD are all possible alternative data sets to test such disease model constructs (Greicius et al., 2003).

Another limitation was the control group used to test for depression specificity. Ideally, an experiment designed with modeling in mind should a priori include a group of controls at least as large as the test subject group. While the control sample examined here did not appear to fit the model, suggesting specificity of the specified circuit for depression, this may be due solely to the small effect size. More optimistically, it is plausible that regions that interact in patients in the resting state reflect tonic maladaptive functional interactions not present in control subjects without a specific stressor. This interpretation is consistent with ongoing studies comparing depressed patients and healthy controls both at rest and during a provoked sad state that demonstrate the attenuation of resting frontal–cingulate path differences between groups with provocation (Liotti et al., 2002; Mayberg, 2002b; Mayberg et al., 2001).

Lastly, studies of depression treatment will be needed to further test the validity of this and similarly described models. Furthermore, with critical nodes identified, further simplification of the model to those paths demonstrating the most significant differences might be additionally examined, potentially increasing parsimony and statistical strength of the fits. Continued development of imaging and multivariate statistical strategies that optimally integrate these factors will be a critical next step in fully characterizing the depression phenotype at the neural systems level with a future goal to develop brain-based algorithms that optimize care of individual depressed patients.

Acknowledgments

The authors thank Steven Brannan MD, J. Arturo Silva MD, and Janet Tekell MD for assessing treatment response in the San Antonio patient group and Craig Easdon, PhD for his assistance with SEM.

References

An, X., Bandler, R., Ongur, D., Price, J.L., 1998. Prefrontal cortical projections to longitudinal columns in the midbrain periaqueductal gray in macaque monkeys. J. Comp. Neurol. 401, 455–479.

Arango, V., Underwood, M.D., Bakalian, M.J., Kassir, S.A., Oppenheim, S., Kelly, T., Dwork, A.J., Mann, J.J., 1999. Reduction in serotonin transporter sites in prefrontal cortex is localized in suicide and widespread in major depression. Abstr.-Soc. Neurosci. 25, 1798.

Auer, D.P., Putz, B., Kraft, E., Lipinski, B., Schill, J., Holsboer, F., 2000. Reduced glutamate in the anterior cingulate cortex in depression: an in vivo proton magnetic resonance spectroscopy study. Biol. Psychiatry 47, 305–313.

Bagby, R.M., Ryder, A.G., Schuller, D.R., 2003. Depressive personality disorder: a critical overview. Curr. Psychiatry Rep. 5, 16–22.

Baxter Jr., L.R., Schwartz, J.M., Phelps, M.E., Mazziotta, J.C., Guze, B.H., Selin, C.E., Gerner, R.H., Sumida, R.M., 1989. Reduction of prefrontal cortex glucose metabolism common to three types of depression. Arch. Gen. Psychiatry 46, 243–250.

Bench, C.J., Friston, K.J., Brown, R.G., Scott, L.C., Frackowiak, R.S., Dolan, R.J., 1992. The anatomy of melancholia-focal abnormalities of cerebral blood flow in major depression. Psychol. Med. 22, 607–615.

Bench, C.J., Friston, K.J., Brown, R.G., Frackowiak, R.S., Dolan, R.J., 1993. Regional cerebral blood flow in depression measured by positron emission tomography: the relationship with clinical dimensions. Psychol. Med. 23, 579–590.

Biver, F., Goldman, S., Delvenne, V., Luxen, A., De Maertelaer, V., Hubain, P., Mendlewicz, J., Lotstra, F., 1994. Frontal and parietal metabolic disturbances in unipolar depression. Biol. Psychiatry 36, 381–388.

Blier, P., Bouchard, C., 1994. Modulation of 5-HT release in the guinea-pig brain following long-term administration of antidepressant drugs. Br. J. Pharmacol. 113, 485–495.

Blier, P., de Montigny, C., 1985. Serotoninergic but not noradrenergic neurons in rat central nervous system adapt to long-term treatment with monoamine oxidase inhibitors. Neuroscience 16, 949–955.

Boomsma, A., 2000. Reporting analyses of covariance structures. Struct. Equ. Modeling 7, 461–783.

Brannan, S.K., Mayberg, H.S., McGinnis, S., Silva, J.A., Mahurin, R.K., Jerabek, P.A., Fox, P.T., 2000. Cingulate metabolism predicts treatment response: a replication. Biol. Psychiatry 47, 107.

Brody, A.L., Saxena, S., Silverman, D.H., Alborzian, S., Fairbanks, L.A., Phelps, M.E., Huang, S.C., Wu, H.M., Maidment, K., Baxter Jr., L.R., 1999. Brain metabolic changes in major depressive disorder from pre- to post-treatment with paroxetine. Psychiatry Res. 91, 127–139.

Brody, A.L., Saxena, S., Stoessel, P., Gillies, L.A., Fairbanks, L.A., Alborzian, S., Phelps, M.E., Huang, S.C., Wu, H.M., Ho, M.L., Ho, M.K., Au, S.C., Maidment, K., Baxter Jr., L.R., 2001. Regional brain metabolic changes in patients with major depression treated with either paroxetine or interpersonal therapy: preliminary findings. Arch. Gen. Psychiatry 58, 631–640.

Buchel, C., Friston, K.J., 1997. Modulation of connectivity in visual pathways by attention: cortical interactions evaluated with structural equation modelling and fMRI. Cereb. Cortex 7, 768–778.

Buchsbaum, M.S., Wu, J., Siegel, B.V., Hackett, E., Trenary, M., Abel, L., Reynolds, C., 1997. Effect of sertraline on regional metabolic rate in patients with affective disorder. Biol. Psychiatry 41, 15–22.

Carmichael, S.T., Price, J.L., 1994. Architectonic subdivision of the orbital

and medial prefrontal cortex in the macaque monkey. J. Comp. Neurol. 346, 366–402.
Carmichael, S.T., Price, J.L., 1995. Limbic connections of the orbital and medial prefrontal cortex in macaque monkeys. J. Comp. Neurol. 363, 615–641.
Caspi, A., Sugden, K., Moffitt, T.E., Taylor, A., Craig, I.W., Harrington, H., McClay, J., Mill, J., Martin, J., Braithwaite, A., Poulton, R., 2003. Influence of life stress on depression: moderation by a polymorphism in the 5-HTT gene. Science 301, 386–389.
Cavada, C., Company, T., Tejedor, J., Cruz-Rizzolo, R.J., Reinoso-Suarez, F., 2000. The anatomical connections of the macaque monkey orbitofrontal cortex. A review. Cereb. Cortex 10, 220–242.
Charara, A., Grace, A.A., 2003. Dopamine receptor subtypes selectively modulate excitatory afferents from the hippocampus and amygdala to rat nucleus accumbens neurons. Neuropsychopharmacology 28, 1412–1421.
Cosgrove, G.R., Rauch, S.L., 1995. Psychosurgery. Neurosurg. Clin. N. Am. 6, 167–176.
Cosgrove, G.R., Rauch, S.L., 2003. Stereotactic cingulotomy. Neurosurg. Clin. N. Am. 14, 225–235.
Damasio, A.R., Grabowski, T.J., Bechara, A., Damasio, H., Ponto, L.L., Parvizi, J., Hichwa, R.D., 2000. Subcortical and cortical brain activity during the feeling of self-generated emotions. Nat. Neurosci. 3, 1049–1056.
Davidson, R., 2001. Toward a biology of personality and emotion. Ann. N. Y. Acad. Sci. 935, 191–207.
Devinsky, O., Morrell, M.J., Vogt, B.A., 1995. Contributions of anterior cingulate cortex to behaviour. Brain 118, 279–306.
Dias, R., Robbins, T.W., Roberts, A.C., 1996. Dissociation in prefrontal cortex of affective and attentional shifts. Nature 380, 69–72.
Dougherty, D.D., Weiss, A.P., Cosgrove, G.R., Alpert, N.M., Cassem, E.H., Nierenberg, A.A., Price, B.H., Mayberg, H.S., Fischman, A.J., Rauch, S.L., 2003. Cerebral metabolic correlates as potential predictors of response to anterior cingulotomy for major depression. J. Neurosurg 99 (6), 1010–1017.
Drevets, W.C., Videen, T.O., Price, J.L., Preskorn, S.H., Carmichael, S.T., Raichle, M.E., 1992. A functional anatomical study of unipolar depression. J. Neurosci. 12, 3628–3641.
Drevets, W.C., Price, J.L., Simpson Jr., J.R., Todd, R.D., Reich, T., Vannier, M., Raichle, M.E., 1997. Subgenual prefrontal cortex abnormalities in mood disorders [see comments]. Nature 386, 824–827.
Duman, R.S., Malberg, J., Thome, J., 1999. Neural plasticity to stress and antidepressant treatment. Biol. Psychiatry 46, 1181–1191.
Elliott, R., 1998. The neuropsychological profile in unipolar depression. Trends Cogn. Sci. 2, 447–454.
Elliott, R., Rubinsztein, J.S., Sahakian, B.J., Dolan, R.J., 2000. Selective attention to emotional stimuli in a verbal go/no-go task, an fMRI study. NeuroReport 11, 1739–1744.
Elliott, R., Rubinsztein, J.S., Sahakian, B.J., Dolan, R.J., 2002. The neural basis of mood-congruent processing biases in depression. Arch. Gen. Psychiatry 59, 597–604.
Ferry, A.T., Ongur, D., An, X., Price, J.L., 2000. Prefrontal cortical projections to the striatum in macaque monkeys: evidence for an organization related to prefrontal networks. J. Comp. Neurol. 425, 447–470.
Fossati, P., Hevenor, S.J., Graham, S.J., Grady, C.L., Keightley, M.L., Craik, F.I., Mayberg, H.S., 2003. In search of the emotional self. A fMRI study using positive and negative emotional words. Am. J. Psychiatry 160, 1938–1945.
Freedman, L.J., Insel, T.R., Smith, Y., 2000. Subcortical projections of area 25 (subgenual cortex) of the macaque monkey. J. Comp. Neurol. 421, 172–188.
Friston, K., 1994. Functional and effective connectivity in neuroimaging: a synthesis. Hum. Brain Mapp. 2, 56–78.
Friston, K.J., Holmes, A.P., Worsley, K.J., Poline, J.-P., Frith, C.D., Frackowiak, R.S.J., 1995. Statistical parametric maps in functional imaging: a general linear approach. Hum. Brain Mapp. 2, 189–210.
George, M.S., Ketter, T.A., Post, R.M., 1994. Prefrontal cortex dysfunction in clinical depression. Depression 2, 59–72.
George, M.S., Ketter, T.A., Parekh, P.I., Horwitz, B., Herscovitch, P., Post, R.M., 1995. Brain activity during transient sadness and happiness in healthy women. Am. J. Psychiatry 152, 341–351.
George, M.S., Ketter, T.A., Parekh, P.I., Rosinsky, N., Ring, H.A., Pazzaglia, P.J., Marangell, L.B., Callahan, A.M., Post, R.M., 1997. Blunted left cingulate activation in mood disorder subjects during a response interference task (the Stroop). J. Neuropsychiatry Clin. Neurosci. 9, 55–63.
Goldapple, K., Segal, Z., Garson, C., Lau, M., Bieling, P., Kennedy, S., Mayberg, H., 2004. Modulation of cortical–limbic pathways in major depression: treatment specific effects of cognitive behavioral therapy compared to paroxetine. Arch. Gen. Psychiatry 61, 34–41.
Greicius, M.D., Krasnow, B., Reiss, A.L., Menon, V., 2003. Functional connectivity in the resting brain: a network analysis of the default mode hypothesis. Proc. Natl. Acad. Sci. U. S. A. 100, 253–258.
Haber, S.N., Kunishio, K., Mizobuchi, M., Lynd-Balta, E., 1995. The orbital and medial prefrontal circuit through the primate basal ganglia. J. Neurosci. 15, 4851–4867.
Harrison, P.J., 2002. The neuropathology of primary mood disorder. Brain 125, 1428–1449.
Heim, C., Nemeroff, C.B., 2001. The role of childhood trauma in the neurobiology of mood and anxiety disorders: preclinical and clinical studies. Biol. Psychiatry 49, 1023–1039.
Henry, M.E., Schmidt, M.E., Matochik, J.A., Stoddard, E.P., Potter, W.Z., 2001. The effects of ECT on brain glucose metabolism: a pilot FDG PET study. J. Ect. 17, 33–40.
Hornig, M., Mozley, P.D., Amsterdam, J.D., 1997. HMPAO SPECT brain imaging in treatment-resistant depression. Prog. Neuro-Psychopharmacol. Biol. Psychiatry. 21, 1097–1114.
Horwitz, B., Tagamets, M.A., McIntosh, A.R., 1999. Neural modeling, functional brain imaging, and cognition. Trends Cogn. Sci. 3, 91–98.
Horwitz, B., Friston, K.J., Taylor, J.G., 2000. Neural modeling and functional brain imaging: an overview. Neural Netw. 13, 829–846.
Hyman, S.E., Nestler, E.J., 1996. Initiation and adaptation: a paradigm for understanding psychotropic drug action. Am. J. Psychiatry 153, 151–162.
Keightley, M.L., Seminowicz, D.A., Bagby, R.M., Costa, P.T., Fossati, P., Mayberg, H.S., 2003. Personality influences limbic–cortical interactions during sad mood induction. NeuroImage 20 (4), 2031–2039.
Kennedy, S.H., Evans, K.R., Kruger, S., Mayberg, H.S., Meyer, J.H., McCann, S., Arifuzzman, A.I., Houle, S., Vaccarino, F.J., 2001. Changes in regional brain glucose metabolism measured with positron emission tomography after paroxetine treatment of major depression. Am. J. Psychiatry 158, 899–905.
Klein, D.F., 1974. Endogenomorphic depression. A conceptual and terminological revision. Arch. Gen. Psychiatry 31, 447–454.
Koob, G.F., Le Moal, M., 2001. Drug addiction, dysregulation of reward, and allostasis. Neuropsychopharmacology 24, 97–129.
Kunishio, K., Haber, S.N., 1994. Primate cingulostriatal projection: limbic striatal versus sensorimotor striatal input. J. Comp. Neurol. 350, 337–356.
Liotti, M., Mayberg, H.S., 2001. The role of functional neuroimaging in the neuropsychology of depression. J. Clin. Exp. Neuropsychol. 23, 121–136.
Liotti, M., Mayberg, H.S., McGinnis, S., Brannan, S.L., Jerabek, P., 2002. Unmasking disease-specific cerebral blood flow abnormalities: mood challenge in patients with remitted unipolar depression. Am. J. Psychiatry 159, 1830–1840.
Malhi, G.S., Bartlett, J.R., 2000. Depression: a role for neurosurgery? Br. J. Neurosurg. 14, 415–422.
Manji, H., Drevets, W., Charner, D., 2001. Neuroimaging and neuropsychological studies of depression: implication for the cognitive-emotion features of mood disorders. Curr. Opin. Neurobiol. 11, 240–249.
Mann, C.D., Vu, T.B., Hrdina, P.D., 1995. Protein kinase C in rat brain cortex and hippocampus: effect of repeated administration of fluoxetine and desipramine. Br. J. Pharmacol. 115, 595–600.

Mann, J.J., Malone, K.M., Diehl, D.J., Perel, J., Cooper, T.B., M.A., M., 1996. Demonstration in vivo of reduced serotonin responsivity in the brain of untreated depressed patients. Am. J. Psychiatry 153, 174–182.

Martinot, J.L., Hardy, P., Feline, A., Huret, J.D., Mazoyer, B., Attar-Levy, D., Pappata, S., Syrota, A., 1990. Left prefrontal glucose hypometabolism in the depressed state: a confirmation. Am. J. Psychiatry 147, 1313–1317.

Mayberg, H.S., 1997. Limbic–cortical dysregulation: a proposed model of depression. J. Neuropsychiatry Clin. Neurosci. 9, 471–481.

Mayberg, H.S., 2002a. Mapping mood: an evolving emphasis on frontal–limbic interactions. In: Stuss, D.T., Knight, R.T. (Eds.), Principles of Frontal Lobe Function. Oxford Univ. Press, New York, pp. 376–391.

Mayberg, H.S., 2002b. Modulating limbic–cortical circuits in depression: targets of antidepressant treatments. Semin. Clin. Neuropsychiatry 7, 255–268.

Mayberg, H.S., 2003. Modulating dysfunctional limbic–cortical circuits in depression: towards development of brain-based algorithms for diagnosis and optimised treatment. Br. Med. Bull. 65, 193–207.

Mayberg, H.S., Lewis, P.J., Regenold, W., Wagner Jr., H.N., 1994. Paralimbic hypoperfusion in unipolar depression. J. Nucl. Med. 35, 929–934.

Mayberg, H.S., Brannan, S.K., Mahurin, R.K., Jerabek, P.A., Brickman, J.S., Tekell, J.L., Silva, J.A., McGinnis, S., Glass, T.G., Martin, C.C., Fox, P.T., 1997. Cingulate function in depression: a potential predictor of treatment response. NeuroReport 8, 1057–1061.

Mayberg, H.S., Liotti, M., Brannan, S.K., McGinnis, S., Mahurin, R.K., Jerabek, P.A., Silva, J.A., Tekell, J.L., Martin, C.C., Lancaster, J.L., Fox, P.T., 1999. Reciprocal limbic–cortical function and negative mood: converging PET findings in depression and normal sadness. Am. J. Psychiatry 156, 675–682.

Mayberg, H.S., Brannan, S.K., Tekell, J.L., Silva, J.A., Mahurin, R.K., McGinnis, S., Jerabek, P.A., 2000. Regional metabolic effects of fluoxetine in major depression: serial changes and relationship to clinical response. Biol. Psychiatry 48, 830–843.

Mayberg, H.S., Westmacott, R., McIntosh, A.R., 2001. A network analysis of trait-state abnormalities. NeuroImage 13, S1071.

McEwen, B.S., 2003. Mood disorders and allostatic load. Biol. Psychiatry 54, 200–207.

McEwen, B.S., Wingfield, J.C., 2003. The concept of allostasis in biology and biomedicine. Horm. Behav. 43, 2–15.

McEwen, B.S., Weiss, J.M., Schwartz, L.S., 1968. Selective retention of corticosterone by limbic structures in rat brain. Nature 220, 911–912.

McIntosh, A.R., 1999. Mapping cognition to the brain through neural interactions. Memory 7, 523–548.

McIntosh, A.R., 2000. Towards a network theory of cognition. Neural Netw. 13, 861–870.

McIntosh, A.R., Gonzalez-Lima, F., 1994. Structural equation modeling and its application to network analysis in functional brain imaging. Hum. Brain Mapp. 2, 2–22.

McIntosh, A.R., Bookstein, F.L., Haxby, J.V., Grady, C.L., 1996. Spatial pattern analysis of functional brain images using partial least squares. NeuroImage 3, 143–157.

Morris, R., Pandya, D.N., Petrides, M., 1999. Fiber system linking the middorsolateral frontal cortex with the retrosplenial/presubicular region in the rhesus monkey. J. Comp. Neurol. 407, 183–192.

Nobler, M.S., Oquendo, M.A., Kegeles, L.S., Malone, K.M., Campbell, C.C., Sackeim, H.A., Mann, J.J., 2001. Decreased regional brain metabolism after ect. Am. J. Psychiatry 158, 305–308.

Nyberg, L., McIntosh, A.R., Cabeza, R., Nilsson, L.G., Houle, S., Habib, R., Tulving, E., 1996. Network analysis of positron emission tomography regional cerebral blood flow data: ensemble inhibition during episodic memory retrieval. J. Neurosci. 16, 3753–3759.

Petrides, M., Pandya, D.N., 1984. Projections to the frontal cortex from the posterior parietal region in the rhesus monkey. J. Comp. Neurol. 228, 105–116.

Petrides, M., Pandya, D., 1994. Comparative architectonic analysis of the human and macaque frontal cortex. In: Boller, G.J. (Ed.), Handbook of Neuropsychology. Elsevier, Amsterdam, pp. 17–58.

Pizzagalli, D., Pascual-Marqui, R.D., Nitschke, J.B., Oakes, T.R., Larson, C.L., Abercrombie, H.C., Schaefer, S.M., Koger, J.V., Benca, R.M., Davidson, R.J., 2001a. Anterior cingulate activity as a predictor of degree of treatment response in major depression: evidence from brain electrical tomography analysis. Am. J. Psychiatry 158, 405–415.

Pizzagalli, D., Pascual-Marqui, R.D., Nitschke, J.B., Oakes, T.R., Larson, C.L., Abercrombie, H.C., Schaefer, S.M., Koger, J.V., Benca, R.M., Davidson, R.J., 2001b. Anterior cingulate activity as a predictor of degree of treatment response in major depression: evidence from brain electrical tomography analysis. Am. J. Psychiatry 158, 405–415.

Plotsky, P.M., Owens, M.J., Nemeroff, C.B., 1998. Psychoneuroendocrinology of depression. Hypothalamic–pituitary–adrenal axis. Psychiatr. Clin. North Am. 21, 293–307.

Rajkowska, G., 2000. Postmortem studies in mood disorders indicate altered numbers of neurons and glial cells. Biol. Psychiatry 48, 766–777.

Ray, J.P., Price, J.L., 1993. The organization of projections from the mediodorsal nucleus of the thalamus to orbital and medial prefrontal cortex in macaque monkeys. J. Comp. Neurol. 337, 1–31.

Sapolsky, R.M., 2000. The possibility of neurotoxicity in the hippocampus in major depression: a primer on neuron death. Biol. Psychiatry 48, 755–765.

Saxena, S., Brody, A.L., Maidment, K.M., Dunkin, J.J., Colgan, M., Alborzian, S., Phelps, M.E., Baxter Jr., L.R., 1999. Localized orbitofrontal and subcortical metabolic changes and predictors of response to paroxetine treatment in obsessive–compulsive disorder. Neuropsychopharmacology 21, 683–693.

Schultz, W., Tremblay, L., Hollerman, J.R., 2000. Reward processing in primate orbitofrontal cortex and basal ganglia. Cereb. Cotex 10, 272–283.

Sheline, Y.I., Wang, P.W., Gado, M.H., Csernansky, J.G., Vannier, M.W., 1996. Hippocampal atrophy in recurrent major depression. Proc. Natl. Acad. Sci. U. S. A. 93, 3908–3913.

Shumake, J., Poremba, A., Edwards, E., Gonzalez-Lima, F., 2000. Congenital helpless rats as a genetic model for cortex metabolism in depression. NeuroReport 11, 3793–3798.

Smith, K.A., Morris, J.S., Friston, K.J., Cowen, P.J., Dolan, R.J., 1999. Brain mechanisms associated with depressive relapse and associated cognitive impairment following acute tryptophan depletion. Br. J. Psychiatry 174, 525–529.

Starkstein, S.E., Robinson, R.G., Price, T.R., 1987. Comparison of cortical and subcortical lesions in the production of poststroke mood disorders. Brain 110, 1045–1059.

Vaidya, V.A., Duman, R.S., 2001. Depression—Emerging insights from neurobiology. Br. Med. Bull. 57, 61–79.

Vogt, B.A., Pandya, D.N., 1987. Cingulate cortex of the rhesus monkey: II. Cortical afferents. J. Comp. Neurol. 262, 271–289.

Vogt, B.A., Finch, D.M., Olson, C.R., 1992. Functional heterogeneity in cingulate cortex: the anterior executive and posterior evaluative regions. Cereb. Cortex 2, 435–443.

Wu, J., Buchsbaum, M.S., Gillin, J.C., Tang, C., Cadwell, S., Wiegand, M., Najafi, A., Klein, E., Hazen, K., Bunney Jr., W.E., Fallon, J.H., Keator, D., 1999. Prediction of antidepressant effects of sleep deprivation by metabolic rates in the ventral anterior cingulate and medial prefrontal cortex. Am. J. Psychiatry 156, 1149–1158.

Zald, D.H., Mattson, D.L., Pardo, J.V., 2002. Brain activity in ventromedial prefrontal cortex correlates with individual differences in negative affect. Proc. Natl. Acad. Sci. U. S. A. 99, 2450–2454.